

Molecular Self-Assembly from Building Blocks Synthesized on a Surface in Ultrahigh Vacuum: Kinetic Control and Topo-Chemical Reactions

Sigrid Weigelt,^{†,§} Christian Bombis,^{†,‡} Carsten Busse,^{†,||} Martin M. Knudsen,[‡] Kurt V. Gothelf,[‡] Erik Lægsgaard,[†] Flemming Besenbacher,[†] and Trolle R. Linderoth^{†,*}

[†]Interdisciplinary Nanoscience Center (iNANO) and Department of Physics and Astronomy, University of Aarhus, Ny Munkegade, DK-8000 Aarhus C, Denmark, and

[‡]Danish National Research Foundation: Centre for DNA Nanotechnology at iNANO and Department of Chemistry, University of Aarhus, 8000 Aarhus C, Denmark. [§]Present address: Nanoscience Centre, University of Cambridge, Cambridge CB3 0FF, United Kingdom. [‡]Present address: Institut für Experimentalphysik, Freie Universität Berlin, D-14195 Berlin, Germany. ^{||}Present address: II. Physikalisches Institut, Universität zu Köln, D-50937 Köln, Germany.

Formation of well-ordered supra-molecular nanostructures on solid surfaces is central to multiple areas and applications within the emerging field of nanotechnology.¹ Molecular self-assembly² from organic compounds deposited onto surfaces by vacuum sublimation has therefore been studied intensively,^{3–8} in particular by the technique of scanning tunneling microscopy (STM), which allows adsorption geometries,⁹ molecular conformations,^{10,11} chirality,^{12–14} and organizational patterns^{3–6,13,14} in the resulting structures to be observed directly. The nucleation and growth of molecular surface structures involves dynamic processes such as diffusion,^{15–17} molecular rotations¹⁸ or conformational changes,^{19,20} and relies on molecular interactions such as hydrogen bonding,⁴ van der Waals (vdW) forces,⁶ or metal complexation.⁸ Molecular self-assembly in general implies formation of structures under equilibrium conditions.² Kinetic effects however can also play an important role in molecular organization on surfaces, if the available thermal energy is insufficient to allow particular dynamic processes or dissociation of nonoptimum molecular aggregates.⁷ This may result, for example, in pronounced effects of changing the deposition order in multicomponent systems²¹ or trapping of metastable structures.²²

As larger and more complex organic molecular building blocks are being employed for surface studies under ultrahigh vacuum (UHV) conditions, a commonly encountered

ABSTRACT Self-assembly of organic molecules on solid surfaces under ultrahigh vacuum conditions has been the focus of intense study, in particular utilizing the technique of scanning tunneling microscopy. The size and complexity of the organic compounds used in such studies are in general limited by thermal decomposition in the necessary vacuum sublimation step. An interesting alternative approach is to deposit smaller molecular precursors, which react with each other on the surface and form the building blocks for the subsequent self-assembly. This has however hitherto not been explored to any significant extent. Here, we perform a condensation reaction between aldehyde and amine precursors codeposited on a Au(111) surface. The reaction product consists of a three-spoke oligo-phenylene-ethynylene backbone with alkyl chains attached through imine coupling. We characterize the self-assembled structures and molecular conformations of the complex reaction product and find that the combined reaction and self-assembly process exhibits pronounced kinetic effects leading to formation of qualitatively different molecular structures depending on the reaction/assembly conditions. At high amine flux/low substrate temperature, compact trimine structures of high conformational order are formed, which inherit organizational motifs from structures formed from one of the reactants. This suggests a topochemical reaction. At low amine flux/high substrate temperature, open porous networks with a high degree of conformational disorder are formed. Both structures are entirely different from that obtained when the trimine product synthesized ex-situ is deposited onto the surface. This demonstrates that the approach of combined self-assembly and on-surface synthesis may allow formation of unique structures that are not obtainable through self-assembly from conventionally deposited building blocks.

KEYWORDS: Molecular self-assembly · scanning tunneling microscopy · imines · oligo-phenylene-ethynylenes · surface reaction

difficulty is thermal fragmentation during the sublimation step. This occurs if the necessary temperature to overcome intermolecular forces exceeds the thermal stability of the compounds themselves. Among the possible solutions²³ to this problem is to synthesize the organic building blocks for the self-assembly directly on the surface from smaller deposited precursors. Nevertheless, in general, the study of organic reactions between adsorbed molecules under

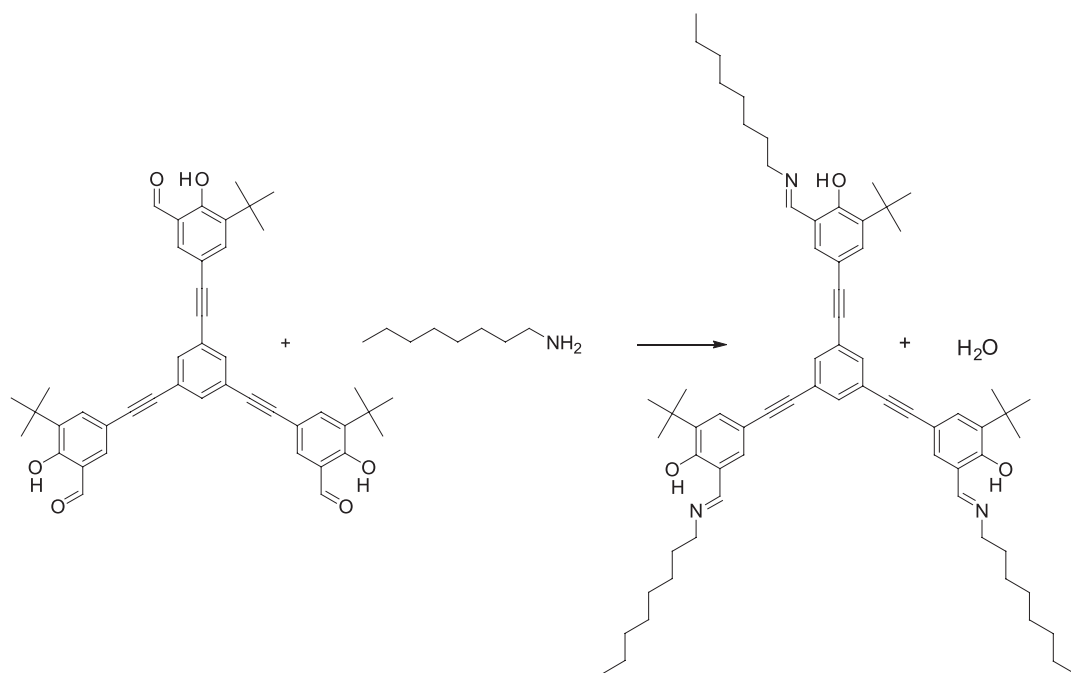
See the accompanying Perspective by Tait on p 617.

*Address correspondence to trolle@phys.au.dk.

Received for review December 20, 2007 and accepted February 06, 2008.

Published online March 19, 2008.
10.1021/nn7004365 CCC: \$40.75

© 2008 American Chemical Society



Scheme 1. Imine formation between a trialdehyde (1,3,5-tris[(5-*t*-butyl-3-formyl-4-hydroxyphenyl)ethynyl]benzene) and octylamine.

extreme UHV conditions has only been pursued to a very limited extent. For instance studies have focused on covalent interlinking induced locally with the tip of an STM^{24–26} or monocomponent polymerizations.^{27–29} Information concerning such a combined on-surface reaction and self-assembly approach is therefore limited.³⁰

We recently took a first step in this direction and demonstrated covalent interlinking between octylamine and aldehyde groups on a two-spoke member of a class of salicylaldehyde functionalized oligo-phenylene-ethynylenes^{31,32} deposited onto the Au(111) surface, resulting in a diimine product.³³ The condensation reaction was confirmed by synchrotron-based X-ray photoelectron spectroscopy and by comparison to the STM imaging signature of the similar reaction product formed *ex-situ* and deposited onto the surface.

Here, we perform a similar surface reaction between a more complex three-spoke oligo-phenylene-ethynylene and octylamine (see Scheme 1) and characterize the molecular conformations and organized structures of the triimine reaction product by high-resolution STM. We find that the resulting structures are critically dependent on the reaction conditions. This demonstrates strong kinetic effects in the combined reaction and surface organization process. At high amine flux and low substrate temperature, amines embed in a matrix formed by preadsorbed three-spoke molecules, which results in compact triimine structures of high conformational order that inherit organizational motifs from the original preassembled structures, suggesting a topochemical reaction.³⁴ At low amine flux and high

substrate temperature, open porous networks are formed with a high degree of conformational disorder in the participating trimines. The underlying dynamic processes, including conformational switching in the compounds even after attachment of the alkyl chains, are investigated by dynamic time-resolved STM. In marked contrast to the situation for the previously studied linear compound, the molecular structures formed after reaction on the surface are completely different from the structure obtained by deposition of the triimine reaction product synthesized *ex-situ*. The present findings offer new insights into the approach of self-assembly after on-surface synthesis and demonstrate that unique structures can be formed that are not obtained by self-assembly from conventionally deposited building blocks.

RESULTS AND DISCUSSION

The three-spoke trialdehyde³¹ reactant (Scheme 1) consists of a central benzene ring connected to three ethynylene spokes separated by 120° angles. Each spoke is connected to a *tert*-butyl substituted salicylaldehyde moiety. Upon vapor sublimation at submonolayer coverage onto the Au(111) surface, the trialdehyde has been observed at temperatures of 140–170 K to form four different, coexisting molecular structures.³¹ Two of these structures, with row- or ladder-type molecular arrangement, are depicted in the high-resolution STM images of Figure 1a,b. The trialdehydes are imaged as Y-shaped entities with bright protrusions at the ends, arising from the *tert*-butyl groups.³¹ The trialdehydes can exist as four different surface conformers, depending on the relative orientation of the

terminal salicylaldehyde moieties.³¹ The conformers can be distinguished in the STM images by the positions of the bright *tert*-butyl groups compared to the molecular backbones. Octylamine forms a densely packed lamellae structure upon deposition at room temperature, as shown in Figure 1c.

In the first preparation procedure trialdehydes were initially dosed onto the Au(111) surface at room temperature (~ 300 K) until a coverage of $\sim 1/3$ of saturation of the first monolayer was reached ($1/3$ ML). The sample was subsequently cooled to a temperature below 170 K, which results in the formation of ordered molecular islands, as described above, and exposed to octylamines ($p \approx 1-5 \times 10^{-7}$ mbar time, 3-5 min), resulting in the growth of octylamine multilayers. After deposition, the sample was briefly annealed to temperatures in the interval between 300 and 400 K to desorb octylamine multilayers and initialize the reaction. Prior to imaging with STM, the sample was again cooled to a temperature between 120 and 170 K to thermally stabilize the resulting product structures. Upon this preparation procedure two coexisting adsorption structures were observed as indicated by "I" and "II" in Figure 2a. The structures have a strong simi-

larity to the ladder- and the row-type structures depicted in Figure 1, and are therefore designated the reacted row and ladder structure. Both the reacted row (Figure 2b,c,d) and the reacted ladder (Figure 2e,f) structure consist of three-spoke backbones adsorbed parallel to the substrate and with the alkyl chains originating from the octylamines extending from the side opposite to the bright *tert*-butyl groups. This STM signature is similar to the situation for the linear aldehydes studied previously,³³ where covalent interlinking was confirmed from spectroscopic measurements. We therefore conclude that the octylamines have reacted with the trialdehydes forming a triimine product.

In the reacted-row structure the ethynylene spokes of the triimines are oriented along the $\langle 11\bar{2} \rangle$ directions and the triimines close-pack pairwise with an end-group of one ethynylene spoke lying in the vertex of

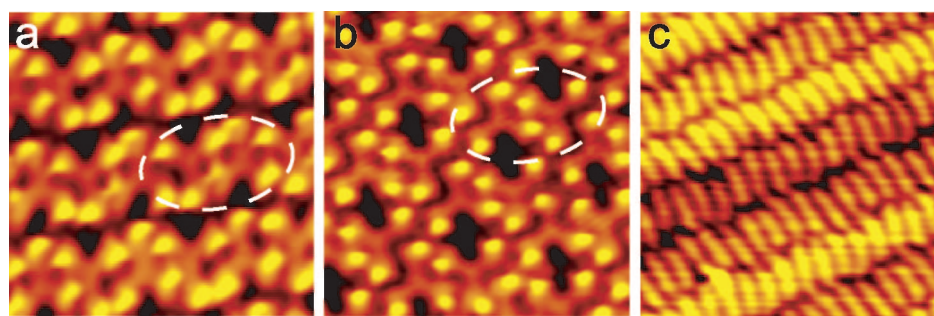


Figure 1. STM images of the reactants (sizes $80 \times 80 \text{ \AA}^2$): (a,b) STM images of the row structure (a) and the open ladder structure (b) formed by the trialdehydes on Au(111).³¹ The ellipses mark characteristic interaction motifs of molecular pairs. In total four different adsorption structures could be found.³¹ (c) Octylamine forms a lamellar structure on Au(111).

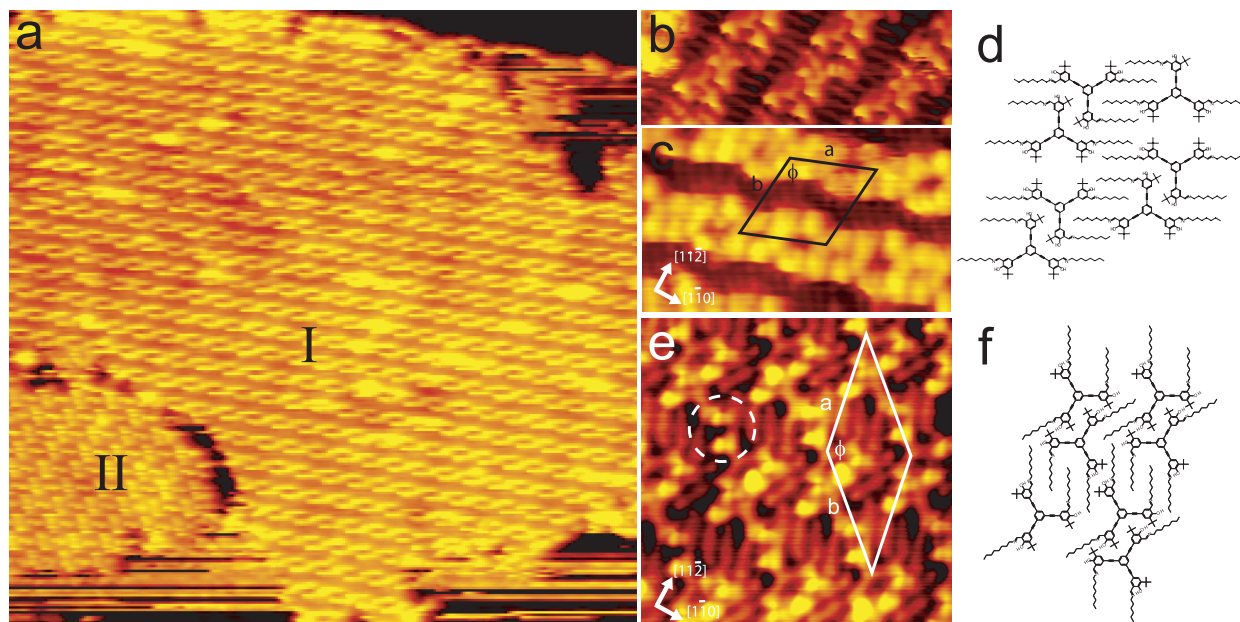


Figure 2. STM images and structural models of triimine structures observed after the preparation procedure involving deposition of octylamine on preassembled islands of trialdehyde reactants. (a) Large-scale STM image of the reacted row (I) and reacted ladder (II) structures (size $850 \times 850 \text{ \AA}^2$, $V_t = 2.4 \text{ V}$, $I_t = 0.33 \text{ nA}$). (b-d) High-resolution STM images and tentative model of the reacted row structure (size $130 \times 50 \text{ \AA}^2$, $V_t = 2.8 \text{ V}$, $I_t = 0.36 \text{ nA}$ /size $150 \times 80 \text{ \AA}^2$, $V_t = 2.3 \text{ V}$, $I_t = 0.38 \text{ nA}$). The unit cell is indicated in (c). (e,f) High-resolution STM image and tentative model of the reacted ladder structure (size $100 \times 100 \text{ \AA}^2$, $V_t = 1.3 \text{ V}$, $I_t = 0.47 \text{ nA}$). The dashed circle marks two molecules joined head-to-head.

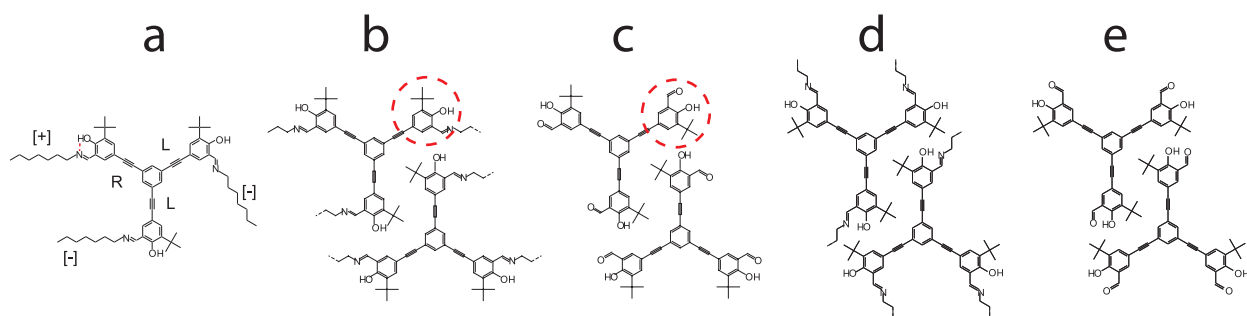


Figure 3. (a) Schematic model showing the different molecular conformations. (b–e) Most favored molecular pairs for the reacted row (b) and ladder (d) structure formed by the triimines, and for the row (c) and open ladder (e) structure formed by the trialdehyde reactants.

the neighboring molecule (see Figure 2b,c). The molecular pairs are arranged into rows with the alkyl chains forming a lamellar motif between the rows. The structure is periodic with a unit cell containing two molecules and with dimensions: $a = (33.4 \pm 1.8) \text{ \AA}$, $b = (36.1 \pm 1.8) \text{ \AA}$, and $\varphi = 117^\circ \pm 5^\circ$.

Also in the reacted ladder structure (Figure 2e,f) the triimines close-pack pairwise with the end-group of one ethynylene spoke lying in the vertex of the pairing molecule. Two molecular pairs are joined head-to-head into extended rows in a configuration where the *tert*-butyl groups (and alkyl chains) point in opposite directions, as indicated with a dashed circle in Figure 2e. The alkyl chains fill out the space between the rows, forming an interwoven structure. The structure is described by a unit cell with dimensions, $a = (41.5 \pm 2.1) \text{ \AA}$, $b = (43.6 \pm 2.2) \text{ \AA}$, and $\varphi = 145^\circ \pm 5^\circ$.

The adsorbed triimines have two conformational degrees of freedom at each molecular spoke (see Figure 3a). First, the salicylaldehyde end-groups can be in two orientations that can be distinguished in the STM images by noting whether the *tert*-butyl groups are to the left (L) or right (R), when looking along the ethynylene spokes from the central benzene ring. Second, the alkyl chains can assume two different orientations designated “+” and “–”. In the “+” configuration the hydroxyl and the imino groups are in sufficient proximity to enable formation of an intramolecular hydrogen bond.

The molecular conformations in the reacted row and ladder structure are very similar as seen from the molecular models in Figures 2d,f. Both structures consist exclusively of molecules with RRL conformation (or LLR in mirror domains) and are thus homochiral. Furthermore, the attached alkyls are in “+” orientation on two of the three molecular spokes. Each molecule thus assumes a configuration allowing for two intramolecular hydrogen bonds. In the reacted-row structure the “–” orientation is observed for the molecular R-spoke (or L-spoke in mirror domains) positioned in the vertex of the pairing molecule. In contrast, molecules in the reacted-ladder structure assume the “–” orientation on the single L-spoke (R-spoke).

There is a striking similarity in the arrangement of triimine backbones in the reacted-row (ladder) structure and the arrangement in the row (ladder) structure for the unreacted trialdehydes,³¹ as can be seen from Figure 1a,b and Figure 3b–e. The molecular pairs in the triimine ladder structure are identical to the molecular pairs in the trialdehyde ladder structure (indicated by an ellipse in Figure 1b). The molecular pairs in the triimine row structure can be realized from the pairs in the trialdehyde row structure (ellipse in Figure 1a) by only one conformational switch around an ethynylene spoke. This allows an all-parallel orientation of the alkyl chains (as indicated with the red dashed circle on the model in Figure 3b,c).

In the second preparation procedure, the Au(111) surface with adsorbed trialdehydes (coverage $\sim 1/3$ ML) was held at room temperature during exposure to octylamines ($p \approx (1-5) \times 10^{-7}$ mbar time, 3–5 min). Subsequently, the sample was briefly annealed to a temperature in the interval between 325 and 450 K to remove unreacted octylamines. Before imaging with STM the sample was cooled to a temperature of 120–170 K. This procedure resulted in the formation of large, ordered porous networks of triimines with pore diameters $d \approx 4$ nm, as shown in the STM images of Figure 4a–c. Only one adsorption structure was observed.

In the porous structure six triimines are arranged in a hexagon with the ethynylene-spokes meeting pairwise head-to-head, as seen in Figures 4b and 4c. Each triimine belongs to three such hexagons, resulting in an extended hexagonal network. The alkyl chains are attached to the aromatic head-groups at the site opposite to the *tert*-butyl group, as expected for the imine reaction product, and are observed to extend into the pores. The ethynylene-spokes are all oriented along a $\langle 1\bar{1}\bar{2} \rangle$ direction. The orientation of the backbones alternates around the pores and the ethynylene spokes of adjacent molecules meet head-to-head (see Figure 4c). The packing of the three-spoke backbones is regular and can be described by a hexagonal unit cell ($\varphi = 120^\circ \pm 3^\circ$) containing two molecules, as marked on the STM images in Figures 4a and 4b. The sides of the unit cell are oriented along $\langle 1\bar{1}\bar{2} \rangle$ directions (deviations $\pm 3^\circ$)

and its dimensions are $a = (39.8 \pm 2.2) \text{ \AA}$, and $b = (39.8 \pm 2.2) \text{ \AA}$.

While the packing of the backbones is regular, the structure is not conformationally ordered, as seen in the STM images of Figure 4b and Figure 4c. Quantitative analysis of high resolution STM images reveals that the four different surface conformations (RRR, RRL, LLR, LLL) of the aromatic backbone are found with nearly equal probability. This implies that the RRL/LLR conformation appears with a lower probability than the probability (3/8) expected for a random distribution (see the table in Figure 4d). Furthermore, most of the trimines have only one out of three alkyl chains in the “+” orientation that enables intramo-

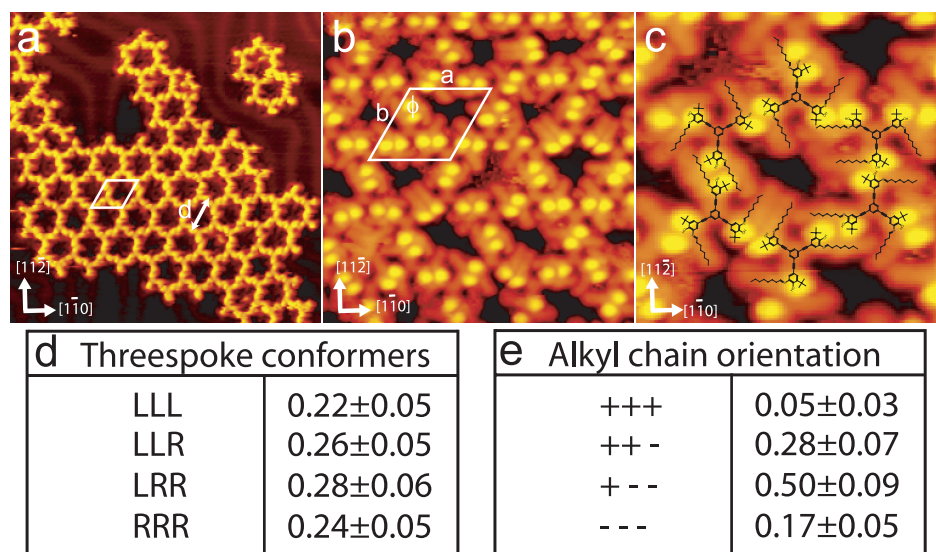


Figure 4. Hexagonal structure obtained after codeposition of octylamine and trialdehyde reactants at room temperature: (a) Large scale STM image of the hexagonal structure obtained in an imaging mode where the aromatic backbone is revealed (size $400 \times 400 \text{ \AA}^2$, $V_t = -1.8 \text{ V}$, $I_t = 0.25 \text{ nA}$); (b) medium scale (size $150 \times 150 \text{ \AA}^2$, $V_t = -1.8 \text{ V}$, $I_t = 0.21 \text{ nA}$); and (c) small scale (size $80 \times 80 \text{ \AA}^2$, $V_t = -1.8 \text{ V}$, $I_t = 0.22 \text{ nA}$) STM images, revealing both alkyl chains and bright *tert*-butyl groups. (d) Distribution of different surface conformations of the trialdehyde backbone. (e) Distribution of alkyl chains on the conformations allowing/not allowing (+/-) an intramolecular hydrogen bond.

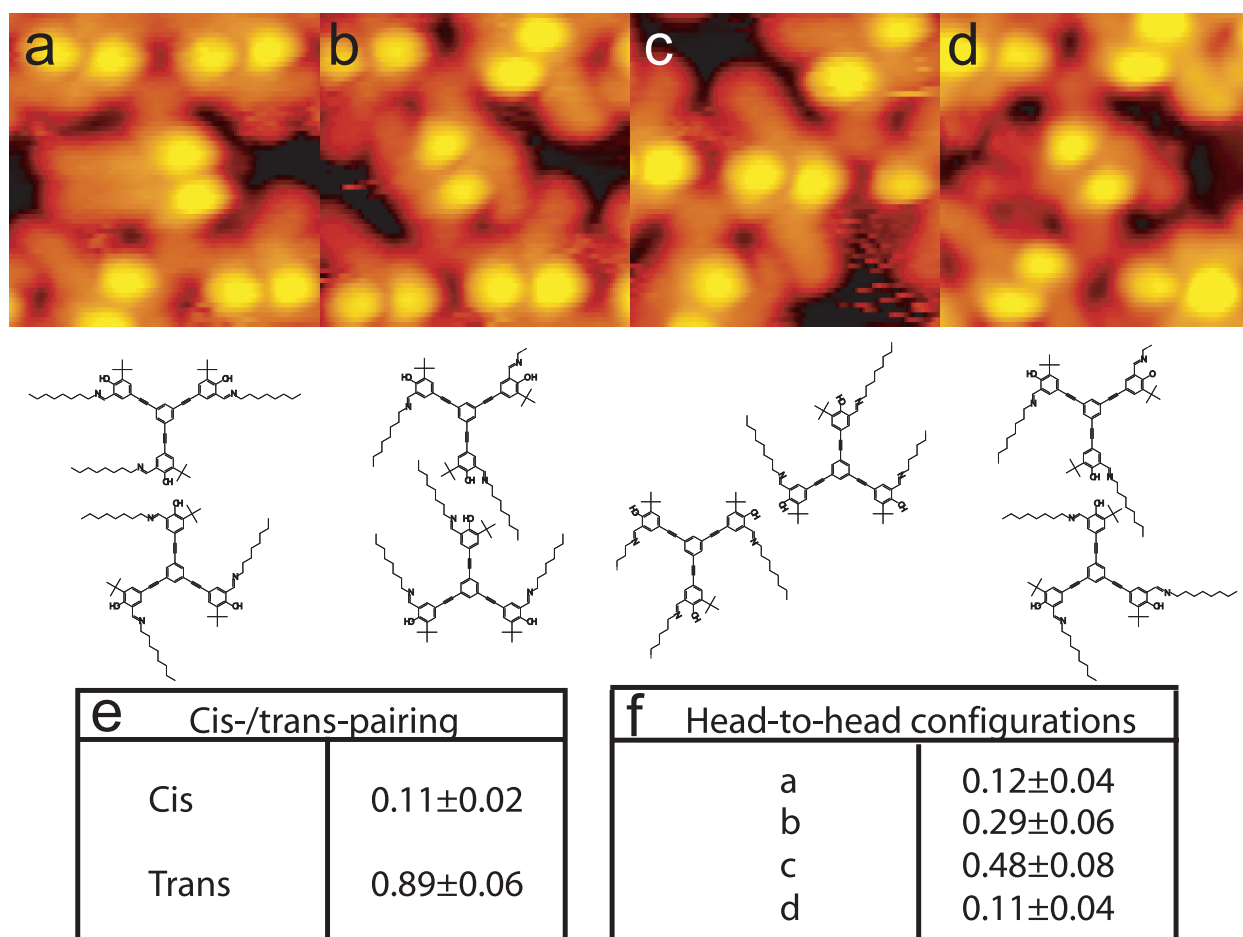


Figure 5. Intermolecular interaction motifs in the hexagonal structure. (a–d) STM images ($40 \times 40 \text{ \AA}^2$) with models below the images. Configuration a constitutes a cis-pairing and b–d are trans-pairings. (e,f) Statistical distribution of the different head-to-head arrangements. Labels a–d refer to the arrangement in the corresponding figure panels.

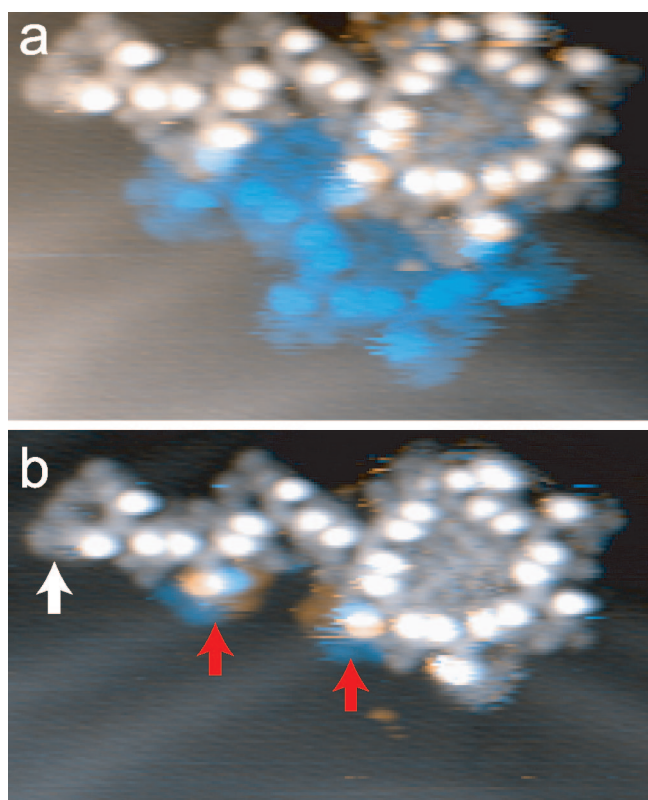


Figure 6. Molecular dynamics at the boundary of the hexagonal structure. In the shown overlays of two STM images, blue/orange color correspond to initial/final configurations ($V_t = -1.8$ V, $I_t = 0.25$ nA): (a) molecules (blue) leaving the island; (b) intramolecular conformational changes. The red arrows mark switches around ethynylene spokes whereby the *tert*-butyl group and alkyl chain interchange positions. The white arrow marks orientational shifts for an alkyl chain.

lecular hydrogen bonding (see the table in Figure 4e). In contrast, for the previously studied diimine,³³ “+” orientations were assumed by all alkyl chains.

The molecular conformations are correlated with the intermolecular arrangements. Two molecules meeting head-to-head around the hexagon, can either assume a configuration in which the *tert*-butyl groups (and alkyl chains) on adjacent molecules point to the same side (Figure 5a) or to opposite sides (Figure 5b,c,d). In accordance with previously used nomenclature we will refer to these intermolecular configurations as *cis* (same side) and *trans* (opposite side).^{19,31} The *cis*/*trans* statistics in Figure 5e stem from analysis of 225 head-to-head pairings counted at images obtained at a temperature between 120 and 147 K. *Trans*-pairing is favored over *cis*-pairing, as also observed for the reactants,^{9,15} the triimines in the ladder structure, and the similar diimine.³³ The energy difference between the favored/unfavored *trans*/*cis* arrangement is 0.02–0.03 eV, as estimated assuming Boltzmann statistics.^{19,31} This is comparable to the situation for structures formed by the aldehyde reactants.^{19,31} Furthermore, the statistics in Figure 5f show that alkyl chains belonging to groups meeting head-to-head preferentially assume the same orientation, with the

configuration in Figure 5c being the most abundant. (The arrangement in Figure 5a is the only sterically allowed *cis* configuration.) Since the alkyl chains are not visible in all STM images, the statistics in the table of Figure 5f are poorer than in the table of Figure 5e.

To obtain insight into the dynamical processes underlying formation of the hexagonal structure, time-lapse STM movies were acquired at a temperature of ~ 168 K. In Figure 6, time-separated STM images are displayed as overlays^{9,15} where blue color tones are used for the first image and orange for the second. This results in stationary features appearing gray, whereas initial (final) positions of a moving feature appears blue (orange). In Figure 6a, molecules at the perimeter of an island (blue) are seen to detach, presumably diffusing out onto the surface. Attachment events are also observed. Since the triimines can both detach and attach to/from the islands at 168 K, we assume that the porous molecular structures are either completely dissolved or in fast dynamic equilibrium with a lattice gas of diffusing molecules at the reaction temperature of ~ 300 K. Alkyl chains attached to molecular backbones at island perimeters are often imaged with a v-shape corresponding to simultaneous imaging of both the “+” and “-” configurations. An example is marked by the white arrow in Figure 6b. This feature is attributed to conformational switching between the “+” and “-” positions, occurring with a rate that is fast compared to that of the STM line scan frequency. The activation energy for the switching process is estimated to be less than 0.4 eV, assuming Arrhenius behavior with a lower limit for the rate of 10 s⁻¹ and a prefactor of 10^{13} s⁻¹. This places an upper bound on the binding strength of a possible hydrogen bond in the “+”-position.³⁵ Similar shifts of alkyl chain orientation are also occasionally observed in the interior of the islands. A final degree of conformational freedom is rotation of the molecular end-groups around the ethynylene spokes, which has previously been observed to occur for the adsorbed trialdehyde reactant.^{19,31} As illustrated by red arrows on the superimposed images of Figure 6b, this switching process also occurs for the triimines, indicating that the alkyl chains do not have a strong bonding to the surface, consistent with the observed high rates for orientational switching of the chains themselves. Similar dynamic events were not observed at a lower temperature of 130 K, indicating that they are indeed thermally activated. Earlier studies of the molecular dynamics inside close-packed islands did not show any influence of the scanning process on the observed dynamics.^{19,31}

The two investigated preparation procedures resulted in formation of qualitatively different self-assembled structures. In the first procedure octylamines were dosed at low temperature unto a substrate pre-covered with trialdehydes. The result was the formation of densely packed structures with complete conformational order. In the second procedure, the substrate

with adsorbed trialdehydes was held at room temperature during sublimation of octylamines onto the surface. The result was an open and less conformationally ordered structure. We tentatively suggest the following scenarios to account for these observations. In the first preparation procedure, octylamine multilayers condense over ordered and stable molecular islands formed from the preadsorbed trialdehydes.³¹ During the subsequent heating ramp, where the octylamine overlayer corresponds to a very high flux of incoming reactants, the octylamines and trialdehydes react to triimines before the structural order of the underlying trialdehyde islands is destroyed. The structures formed have thus inherited organizational motifs from the structurally and conformationally pre-assembled trialdehyde structures. Steric hindrances in the resulting densely packed

arrangement, with an associated high van der Waals attraction, limits or steers conformational changes, resulting in conformational order. Reactions where the products rely on prealignment of the reactants are referred to as topochemically controlled,³⁴ and the molecular organization in the row and ladder structure formed upon preparation 1 are thus presumably steered by topochemical reactions. Since the oligo-phenyleneethynylene backbones are packed denser in the preassembled structures compared to after reaction, the trialdehyde structures must laterally expand to leave space around the molecular pairs for the alkyl chains. In the second procedure, the octylamines are administered at comparatively low flux and at a higher temperature, where the trialdehyde structures are not completely stable. Reaction therefore occurs primarily between species diffusing freely on the substrate, resulting in conformationally unordered triimines. When the substrate temperature is lowered, the products condense into islands of the conformationally unordered hexagonal structure. During this process attachment/detachment at islands and different types of conformational changes are possible, as shown above. It is not *a priori* clear which of the observed structures is thermodynamically favored. The close packed phases formed by the first procedure are likely to be stabilized to the highest extent by attractive vdW interactions, but the

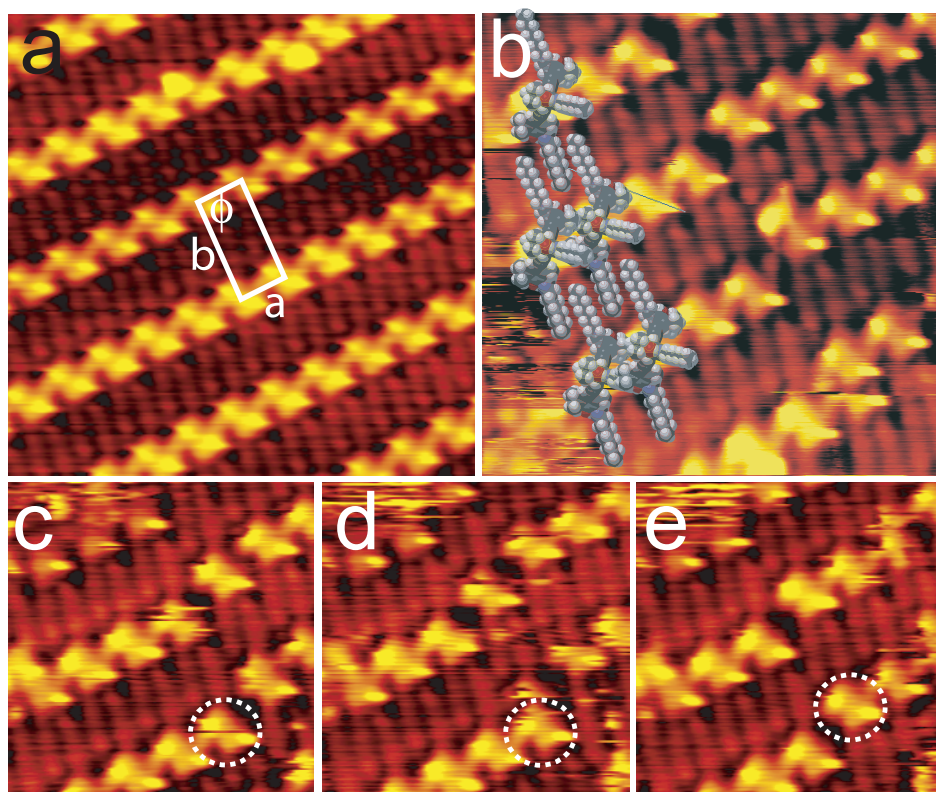


Figure 7. Rectangular structure formed by deposition on the Au(111) surface of triimines synthesized *ex-situ*: (a) STM image of a defect free region (size $120 \times 120 \text{ \AA}^2$, $V_t = 1.6 \text{ V}$, $I_t = 0.57 \text{ nA}$); (b) smaller scale STM image with molecular models superimposed showing the assumed upright adsorption orientation; (c–e) image sequence revealing a moving molecular unit.

conformationally disordered hexagonal structure is favored by entropic effects. Annealing the structures at 400 K did not induce phase transitions from one to the other. This is attributed to kinetically limiting factors such as lack of sufficient thermal energy to dissolve the close-packed phases or problems performing a sufficient number of concerted conformational changes to form the densely packed and conformationally ordered reacted row and ladder structures from freely diffusing species.

It is interesting to compare the structures described above, which are formed from triimines synthesized on the Au(111) surface from deposited molecular precursors, to structures formed by conventional surface self-assembly. For this purpose, triimines were synthesized *ex-situ* by solution phase chemistry.³³ These compounds were subsequently deposited onto the Au(111) surface at $\sim 300 \text{ K}$ by vapor deposition from a glass crucible heated to 390 K. Upon cooling to temperatures of 120–170 K, a single self-assembled structure was observed, as shown in the STM images of Figure 7. This structure is entirely different from the structures described above. It is composed of rows of bright asymmetric protrusions with a lamella arrangement between the rows attributed to the alkyl chains. The structure has a nearly rectangular unit cell with dimensions $a = (11.8 \pm 0.6) \text{ \AA}$, $b = (28.0 \pm 1.4) \text{ \AA}$, and $\phi = 91^\circ \pm 3^\circ$ (see

Figure 7a). We attribute two bright protrusion and two alkyl chains to each molecular entity, since STM movies reveal that such units move in a concerted fashion within the structure (see Figure 7c–d).

The observed molecular units do not conform well with triimines adsorbed with their backbones parallel to the substrate. If instead the triimines are assumed to adsorb in an upright position with one spoke pointing away from the surface, a very good match to the observed structure can indeed be obtained, as shown in Figure 7b. In this adsorption structure, the two bright protrusions correspond to a *tert*-butyl group and the alkyl chain on the upward-pointing molecular headgroup, respectively. The alkyl chains belonging to the two additional spokes form the lamella structure between the rows. It is surprising that the adsorbed triimines do not relax into the flat-lying adsorption orientation observed for the compounds synthesized on the surface. The structure with upright-standing triimines may be stabilized by π -stacking between the aromatic backbones of neighboring molecules, as observed for a similar oligo-phenylene-ethynylene compound.³² Furthermore, triimines with an upright-standing geometry can form three intramolecular hydrogen bonds in contrast to the phases observed for molecules lying down, where only up to two bonds are formed. Upon heating to 400 K the rectangular structure desorbs. In contrast the triimines formed by the on-surface preparation procedures were still found on the surface after heating to temperatures of \sim 450 K. Consequently, the species forming the rectangular structure are bound less strongly to the substrate, which is consistent with a reduced molecule–substrate interaction in the upright-

standing adsorption geometry. An alternative explanation for the observation of a different structure after deposition of triimines synthesized *ex-situ* is that the triimines undergo thermal fragmentation during the sublimation step and that the observed structure is formed by the resulting fragments. However, this latter explanation appears less likely since only one structure is observed and this structure appears to be formed from only one type of molecular entities.

CONCLUSION

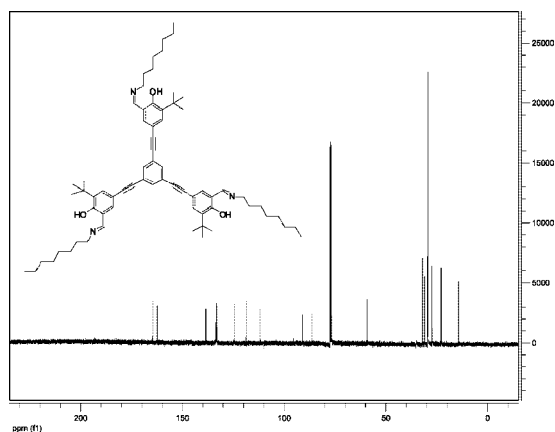
In summary, we have investigated a new approach to self-assembly on surfaces under extremely clean UHV conditions in which large organic building blocks are synthesized on the surface from vacuum-deposited molecular precursors. A strong influence of substrate temperature and reactant flux during the combined reaction and self-assembly process is observed. This offers the possibility of kinetic control of the resulting structures. Conventional surface self-assembly by deposition of the reaction product synthesized *ex-situ* produces entirely different results, suggesting that unique structures may be obtainable by the approach of on-surface synthesis. Of particular interest is the observation that organizational motifs in preassembled structures formed from one of the reactants may be retained in the final product structure. This opens the perspective of future experiments where organized structures formed by weak, reversible self-assembly interactions are subsequently stabilized by stronger, covalent interlinks while retaining their structural order.³⁶

EXPERIMENTAL SECTION

Sample Preparation and STM Measurements. The experiments were performed in an ultrahigh vacuum system equipped with standard facilities for sample preparation and characterization as well as a variable-temperature Aarhus scanning tunneling microscope.³⁷ The Au(111) surface was prepared by repeated cycles of argon-ion sputtering at 1.5 kV followed by annealing to 850 K until the well-ordered ($22 \times \sqrt{3}$) herringbone reconstruction³⁸ was observed by STM. The trialdehydes and presynthesized triimines, which form a solid at room temperature, were evaporated onto the substrate by vapor deposition from a heated glass crucible surrounded by a thin metal wire for resistive heating. Prior to evaporation the powder was thoroughly outgassed at the deposition temperature followed by a brief heating to a slightly higher temperature. During deposition the Au sample was held at room temperature (\sim 300 K). The *n*-octylamine (99%, Aldrich) was held in a glass vial and dosed onto the substrate via a leak valve. Prior to imaging the substrate was cooled to lower temperatures (130–170 K) in the STM.

1,3,5-Tris(5-*tert*-butyl-3-formyl-4-hydroxyphenyl)ethynyl]benzene (Trialdehyde). This compound was prepared as previously described in the literature.³⁹

1,4-Bis(5-*tert*-butyl-4-hydroxy-3-octyliminophenyl)ethynyl]benzene (Triimine). A Schlenk flask containing molecular sieves (100 mg, 3 Å) and a magnetic stirrer bar was dried with a flame under vacuum. 1,3,5-Tris(5-*tert*-butyl-3-formyl-4-hydroxyphenyl)ethynyl]benzene (30 mg, 0.044 mmol), octylamine (0.10 mL, 0.61 mmol), and a catalytic amount of trifluoroacetic acid dissolved in dry CH_2Cl_2 (10 mL) were added and the reaction mixture was stirred at room temperature for 2 h until TLC analysis showed no more starting material left. The mixture was filtered through a pad of celite, diluted with 30 mL of CH_2Cl_2 , and extracted with 15 mL of saturated NH_4Cl . The organic layer was extracted with water (10 mL) and dried (MgSO_4), and the solvent was removed *in vacuo*. The residue was purified by column chromatography (silica gel, 40% CH_2Cl_2 in hexanes, $R_f = 0.30$) to yield 37 mg (85%) of the triimine product as a greenish oil after removal of the solvent. ^1H NMR (400 MHz, CDCl_3): δ 8.30 (s, 3H), 7.60 (s, 3H), 7.48 (s, 3H), 7.32 (s, 3H), 3.60 (t, $J = 6.6$ Hz, 6H), 1.72 (m, 6H), 1.46 (s, 27H), 1.27–1.45 (m, 30H), 0.89 (m, 9H). ^{13}C NMR (100 MHz, CDCl_3): δ 164.7 (3C), 162.4 (3C), 138.5 (3C), 133.5 (3C), 133.3 (3C), 132.9 (3C), 124.5 (3C), 118.6 (3C), 118.6 (3C), 111.7 (3C), 91.0 (3C), 86.3 (3C), 59.3 (3C), 35.2 (3C), 32.1 (3C), 31.0 (3C), 29.5 (3C), 29.4 (6C), 27.4 (3C), 22.9 (3C), 14.4 (3C). MS (MALDI-TOF) *m/e* calcd for $\text{C}_{69}\text{H}_{93}\text{N}_3\text{O}_3$ (M^+), 1011.7; found, 1011.9.



Acknowledgment. We acknowledge financial support from the EU programs FUN-SMART and PICO-INSIDE, as well as from the Carlsberg Foundation, the Danish Technical Research Council, the Danish National Research Foundation and the Danish Natural Science Research Council through funding for the iNANO center. We thank A. H. Thomsen and M. Nielsen for help with synthesis of the molecules.

REFERENCES AND NOTES

- Barth, J. V.; Costantini, G.; Kern, K. Engineering Atomic and Molecular Nanostructures at Surfaces. *Nature* **2005**, *437*, 671–679.
- Whitesides, G. M.; Mathias, J. P.; Seto, C. T. Molecular Self-Assembly and Nanochemistry - a Chemical Strategy for the Synthesis of Nanostructures. *Science* **1991**, *254*, 1312–1319.
- Yokoyama, T.; Yokoyama, S.; Kamikado, T.; Okuno, Y.; Mashiko, S. Selective Assembly on a Surface of Supramolecular Aggregates with Controlled Size and Shape. *Nature* **2001**, *413*, 619–621.
- Theobald, J. A.; Oxtoby, N. S.; Phillips, M. A.; Champness, N. R.; Beton, P. H. Controlling Molecular Deposition and Layer Structure with Supramolecular Surface Assemblies. *Nature* **2003**, *424*, 1029–1031.
- Pawin, G.; Wong, K. L.; Kwon, K. Y.; Bartels, L. A. Homomolecular Porous Network at a Cu(111) Surface. *Science* **2006**, *313*, 961–962.
- de Wild, M.; Berner, S.; Suzuki, H.; Yanagi, H.; Schlettwein, D.; Ivan, S.; Baratoft, A.; Güntherodt, H. J.; Jung, T. A. A Novel Route to Molecular Self-Assembly: Self-Intermixed Monolayer Phases. *Chemphyschem* **2002**, *3*, 881–885.
- Barth, J. V. Molecular Architectonic on Metal Surfaces. *Annu. Rev. Phys. Chem.* **2007**, *58*, 375–407.
- Stepanow, S.; Lingenfelder, M.; Dmitriev, A.; Spillmann, H.; Delvigne, E.; Lin, N.; Deng, X. B.; Cai, C. Z.; Barth, J. V.; Kern, K. Steering Molecular Organization and Host-Guest Interactions using Two-Dimensional Nanoporous Coordination Systems. *Nat. Mater.* **2004**, *3*, 229–233.
- Dougherty, D. B.; Lee, J.; Yates, J. T. Role of Conformation in the Electronic Properties of Chemisorbed Pyridine on Cu(110): An STM/STS Study. *J. Phys. Chem. B* **2006**, *110*, 11991–11996.
- Jung, T. A.; Schlittler, R. R.; Gimzewski, J. K. Conformational Identification of Individual Adsorbed Molecules with the STM. *Nature* **1997**, *386*, 696–698.
- Suzuki, H.; Miki, H.; Yokoyama, S.; Mashiko, S. Identifying Subphthalocyanine Molecule Isomers by Using a Scanning Tunneling Microscope. *J. Phys. Chem. B* **2003**, *107*, 3659–3662.
- Kühnle, A.; Linderroth, T. R.; Hammer, B.; Besenbacher, F. Chiral Recognition in Dimerization of Adsorbed Cysteine Observed by Scanning Tunneling Microscopy. *Nature* **2002**, *415*, 891–893.
- Chen, Q.; Richardson, N. V. Enantiomeric Interactions between Nucleic Acid Bases and Amino Acids on Solid Surfaces. *Nat. Mater.* **2003**, *2*, 324–328.
- Weckesser, J.; Vita, A. D.; Barth, J. V.; Cai, C.; Kern, K. Mesoscopic Correlation of Supramolecular Chirality in One-Dimensional Hydrogen-Bonded Assemblies. *Phys. Rev. Lett.* **2001**, *87*, 096101.
- Schunack, M.; Linderroth, T. R.; Rosei, F.; Lægsgaard, E.; Stensgaard, I.; Besenbacher, F. Long Jumps in the Surface Diffusion of Large Molecules. *Phys. Rev. Lett.* **2002**, *88*, 156102.
- Shirai, Y.; Osgood, A. J.; Zhao, Y. M.; Kelly, K. F.; Tour, J. M. Directional Control in Thermally Driven Single-Molecule Nanocars. *Nano Lett.* **2005**, *5*, 2330–2334.
- Miwa, J. A.; Weigelt, S.; Gersen, H.; Besenbacher, F.; Rosei, F.; Linderroth, T. R. Azobenzene on Cu(110): Adsorption Site-Dependent Diffusion. *J. Am. Chem. Soc.* **2006**, *128*, 3164–3165.
- Stöhr, M.; Wagner, T.; Gabriel, M.; Weyers, B.; Möller, R. Direct Observation of Hindered Eccentric Rotation of an Individual Molecule: Cu-Phthalocyanine on C₆₀. *Phys. Rev. B* **2001**, *65*, 033404.
- Weigelt, S.; Busse, C.; Petersen, L.; Rauls, E.; Hammer, B.; Gothelf, K. V.; Besenbacher, F.; Linderroth, T. R. Chiral Switching by Spontaneous Conformational Change in Adsorbed Organic Molecules. *Nat. Mater.* **2006**, *5*, 112–117.
- Lingenfelder, M.; Tomba, G.; Costantini, G.; Ciacchi, L. C.; De Vita, A.; Kern, K. Tracking the Chiral Recognition of Adsorbed Dipeptides at the Single-Molecule Level. *Angew. Chem., Int. Ed.* **2007**, *46*, 4492–4495.
- Xu, W.; Dong, M. D.; Gersen, H.; Rauls, E.; Vazquez-Campos, S.; Crego-Calama, M.; Reinhoudt, D. N.; Stensgaard, I.; Lægsgaard, E.; Linderroth, T. R.; Besenbacher, F. Cyanuric Acid and Melamine on Au(111): Structure and Energetics of Hydrogen-Bonded Networks. *Small* **2007**, *3*, 854–858.
- Yang, Z. Y.; Zhang, H. M.; Yan, C. J.; Li, S. S.; Yan, H. J.; Song, W. G.; Wan, L. J. Scanning Tunneling Microscopy of the Formation, Transformation, and Property of Oligothiophene Self-Organizations on Graphite and Gold Surfaces. *Proc. Natl. Acad. Sci. U.S.A.* **2007**, *104*, 3707–3712.
- Xu, W.; Dong, M.; Vazquez-Campos, S.; Gersen, H.; Lægsgaard, E.; Stensgaard, I.; Crego-Calama, M.; Reinhoudt, D. N.; Linderroth, T. R.; Besenbacher, F. Enhanced Stability of Large Molecules Vacuum-Sublimated onto Au(111) Achieved by Incorporation of Coordinated Au-Atoms. *J. Am. Chem. Soc.* **2007**, *129*, 10624–10625.
- Okawa, Y.; Aono, M. Materials Science - Nanoscale Control of Chain Polymerization. *Nature* **2001**, *409*, 683–684.
- Hla, S. W.; Bartels, L.; Meyer, G.; Rieder, K. H. Inducing All Steps of a Chemical Reaction with the Scanning Tunneling Microscope Tip: Towards Single Molecule Engineering. *Phys. Rev. Lett.* **2000**, *85*, 2777–2780.
- Ohara, M.; Kim, Y.; Kawai, M. Controlling the Reaction and Motion of a Single Molecule by Vibrational Excitation. *Chem. Phys. Lett.* **2006**, *426*, 357–360.
- Bonello, J. M.; Lambert, R. M.; Kunzle, N.; Baiker, A. Platinum-Catalyzed Enantioselective Hydrogenation of Alpha-Ketoesters: An Unprecedented Surface Reaction of Methyl Pyruvate. *J. Am. Chem. Soc.* **2000**, *122*, 9864–9865.
- Endo, O.; Ootsubo, H.; Toda, N.; Suhara, M.; Ozaki, H.; Mazaki, Y. Phase Transition of a Single Sheet of Sashlike Polydiacetylene Atomic Sash on a Solid Surface. *J. Am. Chem. Soc.* **2004**, *126*, 9894–9895.
- Grill, L.; Dyer, M.; Lafferentz, L.; Persson, M.; Peters, M. V.; Hecht, S. Nano-Architectures by Covalent Assembly of Molecular Building Blocks. *Nat. Nano.* **2007**, *2*, 687–691.
- McCarty, G. S.; Weiss, P. S. Formation and Manipulation of Protopolymer Chains. *J. Am. Chem. Soc.* **2004**, *126*, 16772–16776.
- Busse, C.; Weigelt, S.; Petersen, L.; Lægsgaard, E.; Besenbacher, F.; Linderroth, T. R.; Thomsen, A. H.; Nielsen, M.; Gothelf, K. V. Chiral Ordering and Conformational Dynamics for a Class of Oligo-Phenylene-Ethynyls on Au(111). *J. Phys. Chem. B* **2007**, *111*, 5850–5860.
- Weigelt, S.; Busse, C.; Nielsen, M.; Gothelf, K. V.; Lægsgaard, E.; Besenbacher, F.; Linderroth, T. R. Influence of Molecular Geometry on the Adsorption Orientation for

- Oligophenylene-Ethynyls on Au(111). *J. Phys. Chem. B* **2007**, *111*, 11342–11345.
33. Weigelt, S.; Busse, C.; Bombis, C.; Knudsen, M. M.; Gothelf, K. V.; Strunskus, T.; Wöll, C.; Dahlbom, M.; Hammer, B.; Lægsgaard, E.; Besenbacher, F.; Linderoth, T. R. Covalent Interlinking of an Aldehyde and an Amine on a Au(111) Surface in Ultrahigh Vacuum. *Angew. Chem., Int. Ed.* **2007**, *46*, 9227–9230.
 34. De Feyter, S.; De Schryver, F. C. Two-Dimensional Supramolecular Self-Assembly Probed by Scanning Tunneling Microscopy. *Chem. Soc. Rev.* **2003**, *32*, 139–150.
 35. Mariam, Y. H.; Chantranupong, L. DFT Computational Studies of Intramolecular Hydrogen-Bonding Interactions in a Model System for 5-Iminodaunomycin. *J. Mol. Struct.* **2000**, *529*, 83–97.
 36. Pentecost, C. D.; Peters, A. J.; Chichak, K. S.; Cave, G. W. V.; Cantrill, S. J.; Stoddart, J. F. Chiral Borromeates. *Angew. Chem., Int. Ed.* **2006**, *45*, 4099–4104.
 37. Lægsgaard, E.; Besenbacher, F.; Mortensen, K.; Stensgaard, I. A Fully Automated, 'Thimble-Size' Scanning Tunneling Microscope. *J. Microsc.* **1988**, *152*, 663–669.
 38. Barth, J. V.; Brune, H.; Ertl, G.; Behm, R. J. Scanning Tunneling Microscopy Observations on the Reconstructed Au(111) Surface: Atomic Structure, Long-Range Superstructure, Rotational Domains, and Surface Defects. *Phys. Rev. B* **1990**, *42*, 9307–9318.
 39. Nielsen, M.; Thomsen, A. H.; Jensen, T. R.; Jakobsen, H. J.; Skibsted, J.; Gothelf, K. V. Formation and Structure of Conjugated Salen-Cross-Linked Polymers and their Application in Asymmetric Heterogeneous Catalysis. *Eur. J. Org. Chem.* **2005**, 342–347.